Math. Model. Nat. Phenom. 19 (2024) 8
https://doi.org/10.1051/mmnp/2024006

Mathematical Modelling of Natural Phenomena
www.mmnp-journal.org

ADDITIVE MULTIPLE CONTACTS AND SATURATION PHENOMENA IN EPIDEMIOLOGICAL MODELS ARE NOT DETECTED BY R_0

José Geiser Villavicencio-Pulido[1,*], Ignacio Barradas[2] and Claudia Nila-Luévano[3]

Abstract. Many infections are transmitted by direct contacts. Usually, one single direct contact is needed to transmit the required minimum infectious load. Most models describe contagions by single contacts using a term of the type mass action law. However, modelling infections that are transmitted after the susceptible individual had contact with several sources of infection requires more than mass action law terms. We call additive multiple contacts those that do not produce infection by themselves, but can produce infection if they happen simultaneously. We are interested in understanding the role played by R_0 missing the mark in infections in which the minimum infectious load is reached not only by single contacts but also by additive multiple contacts. We propose different mathematical models describing not only infections by one single contact but also by additive multiple contacts. We show that all models have the same value of R_0, but correspond to different epidemiological mechanisms. Two models show contagions by additive multiple contacts and a third one shows reduction of infections by some saturation process which is not captured by R_0. This shows that trying to control the epidemics by controlling R_0 could be unsufficient or, in some cases, waste resources.

Mathematics Subject Classification. 92B05, 92D30, 34C60, 35F25.

Received March 23, 2023. Accepted March 23, 2024.

1. Introduction

Epidemiological mathematical models are nowadays more important than ever. There are plenty of efforts to construct models that faithfully describe the evolution of an epidemic. Most models are established by modular adding of terms in a difference or differential equation. In these models, it is sought that the terms involved capture particular phenomenologies of each disease.

The most common term for describing infections is the mass action law. The term βSI describes the number of new infections per unit of time that occur due to encounters between susceptible and infectious individuals. The term βSI describes the cases for which the infectious load is reached by a single contact with an infectious

Keywords and phrases: Additive multiple contacts, SARS-CoV-2, COVID-19, epidemic model, public health strategies, parameter estimation.

[1] Universidad Autónoma Metropolitana, Av. Hidalgo Poniente No. 46, Col. La Estación, 52006, Lerma de Villada, Estado de México, Mexico.
[2] Centro de Investigación en Matemáticas, 36023 Guanajuato, Guanajuato, Mexico.
[3] Independent researcher.

* Corresponding author: j.villavicencio@correo.ler.uam.mx

individual. Therefore, the term βSI models the assumption that given a contact, only a factor describing the probability of such contact turning into an actual infection is needed.

If we call an effective contact one in which one single individual is able to transfer the minimum infectious load, the mass action law does capture it accurately. A scenario in which two or more simultaneous contacts are required for the transference of the minimum infectious load is not included in this term.

Even though it is common that mathematical models still consider only one-time encounters with infected people and it is assumed that the minimum infectious load is reached in one single event. What if the total load to start an infection is acquired not only by a single contact but also by several additive contacts? Is R_0 able to capture this epidemiological mechanism? Would that affect our control strategies?

The minimum infectious load varies from disease to disease. There are however many examples of pathogens that have to overcome a minimum threshold to be able to successfully settle down in a host [1]. Shigella and Giardia lamblia, for example, require about 10 cells to start an infection [2], while Vibrio cholerae and Staphylococcus aureus require 10^3–10^8 cells in order to develop an infection. A review of the minimum infective load for COVID-19 in humans can be found in [3]. The authors suggest that the minimum infective load in humans for SARS-CoV-2 is around one hundred viruses. This estimation was based on computational simulations of nasopharynx during the transmission and inhalation of droplets [4]. So, even for Covid-19 some minimum load is required for infection to develop. Many other pathogens infect under similar constraints of a minimum load that has to be overcomed to be considered an effective infection [5]. This minimum load can be obtained during several almost simultaneous encounters. So, the infection process can be seen as additive.

We want to point out that the minimum infectious load might be reached not only by single contacts but also by additive multiple contacts, and this can be relevant for control measures when these relay only on values of R_0. Whenever we talk about additive multiple contacts in this work we are referring to those contacts with different sources (different individuals or individual-environmental) that are needed to reach the minimum infectious load. We assume that each single contact of this kind is not able to produce the disease by itself, two or more contacts add up to reach the load required for developing the disease. Then, infectious diseases in which new contagions occur not only for single contacts but also for additive multiple contacts must be modeled with the term βSI to describe single contagions and with higher order terms like βSI^2 to describe contagions in which the minimum infectious load is reached in several simultaneous contacts. Terms of the form βSI^2 can be interpreted as the (almost) simultaneous encounters of three individuals. In the case of infections, this could be, for example, two infectious individuals close to a susceptible one, providing each a fraction of the necessary minimum infectious load. Of special interest are airborne diseases, for which there is enough evidence that being in close proximity in restaurants, churches, and similar places allows the pathogen to produce an effective infection [6]. The pathogen in the air could come from two different individuals. In such a case, two infected individuals coughing next to a susceptible person could be considered multiple exposures. This term does not include the cases for which one single individual provides the minimum infectious load, those would be included in term βSI. In an analogous way, depending on who is spreading the pathogen, other terms to the power two can be considered. This kind of terms can also describe other interactions and phenomena; see [7]. Notice that higher order terms are sometimes inadvertently included or missed when infections by single and multiple additive contacts are modeled using nonlinear infection forces [8–11].

A usual control strategy for diseases is to look for values of R_0 and to bring it below 1. But if R_0 considers only direct single contacts, as we will show, any increment induced by higher order contacts might be relevant and is neglected in such calculations [12]. In this case, any control strategy based on reducing R_0 might be insufficient. For any control measure to really work, not only the well-known case of backward bifurcation (see [8–10, 13]) has to be considered, but also the fact that infections by additive multiple contacts could increase the actual number of total infections in a way that makes the epidemic self-sustained due to the existence of multiple endemic equilibria even when R_0 is smaller than one. This means that, especially for values of R_0 close to 1, it is important to evaluate the effect of additive multiple contacts and they should be considered in some models.

We present different models describing contagions not only for single contacts but also for additive multiple contacts. The proposed models capture both human-to-human contagions and contaminated-environment-to-human contagions [14–17]. Through these models, we show that the evolution of infectious diseases can have totally different dynamics when the model considers not only contagions by single contacts but also by additive multiple contacts. Even more, we show that the basic reproduction number, R_0, can underestimate or overestimate the number of secondary infections, which could lead to the design of deficient control strategies from an epidemiological or economical point of view. In Section 2.10, the epidemic models are presented and qualitative analysis of the solutions of the models are performed. In Section 3, epidemiological parameters are estimated for each model using published data for confirmed cases of infections by SARS-CoV-2 in Mexico. In Section 4, numerical simulations of the solutions of the analyzed models are shown. Finally, in Section 5, we discuss the results of the analysis of the models.

2. The models and R_0

In this section, we illustrate the main shortcomings of the use of mass action law for properly capturing additive multiple contacts. We discuss the model presented in [18], and analyze two additional models (2.1) and (2.14). The general hypotheses for all three models are the same. The only difference is that Yang's model describes infections only by single contacts, that is, it considers only the mass action law. In contrast, models (2.1) and (2.14) include the mass action law as well as infections due to additive multiple contacts.

We will establish that all three models share the same R_0. Nevertheless, the dynamics of each one will present crucial differences.

In the models proposed, (2.1) and (2.14), we consider two infection pathways: human-to-human and environment-to-human. The total population is divided into four epidemiological classes: the susceptible individuals, the exposed, the infected, and the recovered ones, which are denoted by S, E, I, and R, respectively. Exposed individuals that are in the incubation period, and will eventually develop full symptomatology, are in the E class. Infected individuals that have fully developed symptoms are in the I class. Notice that the models include the possibility that exposed individuals might also be infectious in a certain way. The pathogen concentration in the environmental reservoir is denoted by V. Observe that, if double additive contacts are not taken into account, our models coincide with the model proposed in Yang and Wang (2020) [18].

2.1. Infections as result of additive multiple contacts: first model

Here we propose a first model describing infections by single contacts as well as by additive multiple contacts. We assume that in the case of infections by additive multiple contacts, two contacts are required for the transference of the minimum infectious load. Particularly, we model the scenario in which infections by additive multiple contacts increase without bound as a function of the contagious agent. In model (2.14), these interactions will be considered to be bounded.

The starting model is

$$\begin{aligned} \dot{S} &= \Lambda - \kappa_1 SE - \kappa_2 SI - \kappa_3 SV - F_1(E,I,V)S - \mu S, \\ \dot{E} &= \kappa_1 SE + \kappa_2 SI + \kappa_3 SV + F_1(E,I,V)S - (\alpha+\mu)E, \\ \dot{I} &= \alpha E - \omega_1 I, \\ \dot{R} &= \gamma I - \mu R, \\ \dot{V} &= \xi_1 E + \xi_2 I - \sigma V. \end{aligned} \tag{2.1}$$

With $\omega_1 = (\omega + \gamma + \mu)$ and

$$F_1(E,I,V) = \phi_1 E^2 + \phi_2 I^2 + \phi_3 V^2 + \phi_4 EI + \phi_5 EV + \phi_6 IV. \tag{2.2}$$

The parameter Λ is the recruitment rate of susceptible individuals, α^{-1} is the mean incubation period, ω is the disease-related death rate, γ is the recovery rate, μ is the natural death rate of the human host. The parameters ξ_1 and ξ_2 are the releasing rates of virus to the environmental reservoir by the exposed individuals and symptomatic ones. σ is the clearance rate of free virus from the environment.

In model (2.1), the number of new infected individuals is modeled by

$$\kappa_1 SE + \kappa_2 SI + \kappa_3 SV + F_1(E, I, V)S. \tag{2.3}$$

$$G(E, I, V) = \kappa_1 E + \kappa_2 I + \kappa_3 V + F_1(E, I, V). \tag{2.4}$$

The force of infection $G(E, I, V)$ is a function of both infections by single contacts as well as by additive multiple contacts.

In (2.4), κ_1 is the product of the average number of single contacts between exposed individuals, and susceptible ones per unit of time, multiplied by the probability that those single encounters result in new infections. κ_2 is defined in a similar way for the infectious individuals. κ_3 is the average number of single contacts between susceptible individuals and contaminated surfaces, multiplied by the probability that those single encounters result in new infections. The effective contact rates involved in $F_1(E, I, V)$ are described as follows. ϕ_1 (and ϕ_2) is the product of the average number of two contacts among exposed (infectious) individuals and susceptible ones per unit of time, multiplied by the probability that those encounters result in new infections. That is, ϕ_1 and ϕ_2 measure the number of new infections due to additive multiple contacts of susceptible individuals with exposed individuals or infectious ones, respectively. In an analogous way, ϕ_3 measures the number of new infections due to additive multiple contacts of susceptible individuals with two fomites resources. Each ϕ_4, ϕ_5 and ϕ_6 is the product of the average number of two contacts among the different infectious sources, E, I, and V, and susceptible ones per unit of time, multiplied by the probability of those encounters results in new infections. Then, κ_i measures the new infectious due to single contacts, while ϕ_j measures the new infectious due to additive multiple contacts, for $i = 1, 2, 3$ and $j = 1, 2, 3, 4, 5, 6$; see [8, 19, 20].

For model (2.1), the basic reproduction number is

$$R_0 = R_0^E + R_0^I, \tag{2.5}$$

with

$$R_0^E = \frac{S_0}{(\alpha+\mu)}\left(\kappa_1 + \frac{\kappa_3\xi_1}{\sigma}\right) \quad \text{and} \quad R_0^I = \frac{\alpha S_0}{(\omega_1(\alpha+\mu))}\left(\kappa_2 + \frac{\kappa_3\xi_2}{\sigma}\right), \tag{2.6}$$

R_0 was calculated using the next generation matrix [21, 22]. In expression (2.5), R_0^E is the contribution of exposed individuals to the production of new infections while R_0^I is the contribution of infectious individuals to the production of new infections. Each term of (2.5) considers the environment-to-human transmission route for virus released by exposed individuals or infectious individuals, respectively.

The basic reproduction number associated with model (2.1), according to (2.5), is equal to R_0 calculated in [18]. This result is unexpected because Yang's model [18] describes a reduction in the number of new contagions due to an increase in the number of symptomatic infectious individuals, while model (2.1) describes an increase in the number of new contagions due to an increase in the number not only of symptomatic individuals but also of exposed individuals and viruses in the environment. Misunderstanding the real number of new infections must be seen a red flag of the fact that the basic reproduction number overlooks infections which can be relevant from a control or economic perspective.

Moreover, if we calculate the basic reproduction number of a simplified version of model (2.1), one in which infections produced by multiple additive contacts are not considered and we only consider infections produced by single contacts, the basic reproduction number is again the same as model (2.1) and Yang's model. That is, the basic reproduction number is the same for the three models: model only considering infections by single

contacts (model (2.1) with $\phi_j = 0$, for $j = 1, 2, 3, 4, 5, 6$); model only considering infections by single contacts which decrease when the pathogen agent increases (model (2.1) in [18]) and model that considers not only infections by single contact but also infections by multiple contacts that also increase when the pathogen agent increases (model (2.1)). Then, the value calculated of R_0 (that coincides with the case in which the additive multiple contacts are not considered) should overestimate the value of the basic reproduction number for model (2.1) in [18] (that describes a decreasing in the infectious rate) and it underestimates the value of the basic reproduction number for model (2.1) in which there are modeled contagions by additive multiple contacts.

In Section 2.3 we will consider an additional model, equations (2.14), which will again have the same R_0 associated, despite the fact that it describes a totally different dynamics.

In the following, we analyze the existence of equilibria points for model (2.1).

2.2. Equilibria solutions for model (2.1)

Now, we analyze the existence of equilibrium points for model (2.1). By definition, $X^* = (S^*, E^*, I^*, R^*, V^*)$ is an equilibrium point of system (2.1) if and only if the vector field associated to model (2.1) is null. Then we have to solve the following nonlinear system.

$$\begin{aligned}
&\Lambda - \kappa_1 S^* E^* - \kappa_2 S^* I^* - \kappa_3 S^* V^* - F_1(E^*, I^*, V^*) - \mu S = 0,\\
&\kappa_1 S^* E^* + \kappa_2 S^* I^* + \kappa_3 S^* V^* + F_1(E^*, I^*, V^*) - (\alpha + \mu) E^* = 0,\\
&\alpha E^* - \omega_1 I^* = 0,\\
&\gamma I^* - \mu R^* = 0,\\
&\xi_1 E^* + \xi_2 I^* - \sigma V^* = 0.
\end{aligned} \tag{2.7}$$

Solving the last three equations of system (2.7) as functions of the variable I^* yields

$$\begin{aligned}
E^* &= \tfrac{\omega_1}{\alpha} I^*,\\
R^* &= \tfrac{\gamma}{\mu} I^*,\\
V^* &= \tfrac{\omega_1 \xi_1 + \alpha \xi_2}{\sigma \alpha} I^*.
\end{aligned} \tag{2.8}$$

The equilibrium value of S^* as a function of I^* is found using the first two equations of (2.7). Then

$$S_1(I^*) = \frac{1}{\mu}\left(\Lambda - \delta_0 I^*\right), \tag{2.9}$$

with $\delta_0 = \frac{\omega_1(\alpha+\mu)}{\alpha}$.

Now, using the second equation of (2.7) and substituting the values of the variables E^*, I^*, R^* yield

$$S_2(I^*) = \frac{\delta_1}{\delta_2 I^* + \delta_3}, \tag{2.10}$$

with

$$\begin{aligned}
\delta_1 &= (\alpha+\mu)\,\omega_1\alpha\,\sigma^2,\\
\delta_2 &= (\alpha\,\xi_2+\xi_1\omega_1)^2\,\phi_3+\sigma^2\left(\phi_2\alpha^2+\phi_1{\omega_1}^2\right)+\delta_4,\\
\delta_3 &= \alpha\,\sigma\,\left((\xi_1\omega_1+\xi_2\alpha)\,\kappa_3+\sigma\,(\kappa_1\omega_1+\alpha\,\kappa_2)\right),\\
\delta_4 &= \sigma\,\phi_4\omega_1\alpha+\sigma\,\left(\left({\omega_1}^2\xi_1+\omega_1\xi_2\alpha\right)\phi_5+\left(\alpha\,\xi_1\omega_1+\alpha^2\xi_2\right)\phi_6\right).
\end{aligned} \tag{2.11}$$

Observe that if $\phi_j=0$ for $j=1,2,3,4,5,6$, $S_2(I^*)$ is a constant function.

The disease-free equilibrium point for model (2.1) is $E_0=\left(\frac{\Lambda}{\mu},0,0,0,0\right)$. The endemic equilibrium points of system (2.1) are the intersection points of the curves $S_1(I^*)$ and $S_2(I^*)$, for $I^*>0$. We analyze the behavior of these functions to prove the existence of endemic equilibrium points.

Calculating the derivatives of first and second order of $S_1(I^*)$ and $S_2(I^*)$ we obtain

$$\begin{aligned}
\tfrac{dS_1(I^*)}{dI^*} &= -\delta_0,\\
\tfrac{d^2S_1(I^*)}{{dI^*}^2} &= 0,\\
\tfrac{dS_2(I^*)}{dI^*} &= -\tfrac{\delta_1\delta_2}{(\delta_2I^*+\delta_3)^2},\\
\tfrac{d^2S_2(I^*)}{{dI^*}^2} &= 2\,\tfrac{\delta_1{\delta_2}^2}{(\delta_2I^*+\delta_3)^3}.
\end{aligned}$$

The nontrivial equilibrium points are given by the intersection of the linear function $S_1(I^*)$ and the convex function $S_2(I^*)$.

The nullclines $S_1(I^*)$ and $S_2(I^*)$ satisfy

$S_1(0)=\frac{\Lambda}{\mu}\equiv S_0$, $S_1\left(\frac{\Lambda\,\alpha}{\omega_1(\alpha+\mu)}\right)=0$, $S_2(0)=\frac{S_0}{R_0}$ and $\lim\limits_{I^*\to\infty}S_2(I^*)=0$.

Then

- If $R_0=1$, then $S_1(0)=S_2(0)$.
- If $R_0<1$, then $S_1(0)<S_2(0)$.
- If $R_0>1$, then $S_1(0)>S_2(0)$.

We define the function $O(I^*)=\frac{dS_2(I^*)}{dI^*}-\frac{dS_1(I^*)}{dI^*}$.
Then, $O(0)=\frac{\delta_0\left(-\delta_2\alpha^2\mu\,\sigma^2+{\delta_3}^2\right)}{{\delta_3}^2}<0 \iff \frac{\delta_2\alpha^2\mu\,\sigma^2}{{\delta_3}^2}>1$.

$O(I^*)$ is an increasing function of I^*, and $\lim\limits_{I^*\to\infty}O(I^*)=\delta_0>0$.

Furthermore, there is a unique I_c^* such that $O(I_c^*)=0$. That is, $S_1(I^*)$ and $S_2(I^*)$ have the same derivative in I_c^*. Assume that $R_0<1$ and there are no intersection points of $S_1(I^*)$ and $S_2(I^*)$. If R_0 increases until a certain

value of R_0, which we will call R_0^*, then $S_2(I^*)$ touches $S_1(I^*)$ tangentially in I_c^*. After that, the tangential point I_c^* bifurcates in two points that are intersection points of $S_1(I^*)$ and $S_2(I^*)$, which are denoted by I_I^* and I_2^*. Additionally, $I_1^* < I_2^*$ until I_1^* disappears and $I_2(I^*)$ is the unique equilibrium point that exists for all $R_0 > 1$.

We can summarize the previous analysis in the following results: Theorem 2.1 for $\frac{\delta_2 \alpha^2 \mu \sigma^2}{{\delta_3}^2} > 1$, and Theorem 2.2 for $\frac{\delta_2 \alpha^2 \mu \sigma^2}{{\delta_3}^2} < 1$.

Theorem 2.1. *For model (2.1), the value of R_0 is given by $R_0 = \frac{\kappa_1}{\alpha+\mu} S_0 + \frac{\kappa_2 \alpha}{\omega_1(\alpha+\mu)} S_0 + \frac{\kappa_3(\xi_1\omega_1+\xi_2\alpha)}{\sigma\omega_1(\alpha+\mu)} S_0$. Additionally, if*

$$\frac{\delta_2 \alpha^2 \mu \sigma^2}{{\delta_3}^2} > 1, \tag{2.12}$$

then there exists a value $R_0^* \in (0,1)$ such that

a) If $R_0 < R_0^*$, then there are no non trivial endemic equilibrium points.
b) If $R_0 = R_0^*$, then there is one single non trivial equilibrium, which is a saddle point.
c) If $R_0^* < R_0 < 1$, then there are two non trivial endemic equilibrium points.
d) If $R_0 \geq 1$ there is one non trivial endemic equilibrium point.

Condition (2.12) indicates for model (2.1) how each parameter contributes to the appearance or absence of a backward bifurcation.

Note that getting rid of double exposures in model (2.1) is equivalent to letting $\phi_j = 0$, for $j = 1, 2, 3, 4, 5, 6$, which in turn makes $\delta_2 = 0$. This at some point guaranties $\frac{\delta_2 \alpha^2 \mu \sigma^2}{{\delta_3}^2} < 1$, which is equivalent to $R_0^* = 1$. That is, cases b) and c) in Theorem 2.1 disappear and case d) holds true only for the strict inequality. By the same token Yang's model does not present backward bifurcation either.

Even though it is not usual to have explicit coordinates for I^*, this case is an exception. For model (2.1), the values for the variable I at the equilibrium points are given by

$$I^* = \frac{-B \pm \sqrt{B^2 - 4AC}}{2A}. \tag{2.13}$$

With

$$\begin{aligned}
A &= \omega_1 (A_1 + A_2)(\alpha + \mu), \\
B &= \alpha (B_1 + B_2 + B_3), \\
C &= \alpha^2 \sigma^2 \omega_1 \mu (\alpha + \mu)(1 - R_0), \\
A_1 &= (\xi_1\omega_1 + \xi_2\alpha)^2 \phi_3, \\
A_2 &= \sigma \left((\xi_1\omega_1 + \xi_2\alpha)(\alpha\phi_6 + \omega_1\phi_5) + \sigma \left(\phi_2\alpha^2 + \alpha\phi_4\omega_1 + \phi_1{\omega_1}^2 \right) \right), \\
B_1 &= \omega_1\sigma (\xi_1\omega_1 + \xi_2\alpha)(\alpha + \mu)\kappa_3, \\
B_2 &= -\Lambda (\xi_1\omega_1 + \xi_2\alpha)((\xi_1\omega_1 + \xi_2\alpha)\phi_3 + \alpha\sigma\phi_6 + \omega_1\sigma\phi_5), \\
B_3 &= \omega_1\sigma^2 (\kappa_1\omega_1 + \alpha\kappa_2)(\alpha + \mu) - \Lambda\sigma^2 \left(\phi_2\alpha^2 + \alpha\phi_4\omega_1 + \phi_1{\omega_1}^2 \right).
\end{aligned}$$

Substituting (2.13) in expressions (2.8) and (2.9) the endemic equilibria points for model (2.1) are obtained. Inverting condition (2.12), the following result can be proved.

Theorem 2.2. *For model (2.1).*
If $\frac{\delta_2 \alpha^2 \mu \sigma^2}{{\delta_3}^2} < 1$, model (2.1) shows a forward bifurcation at $R_0 = 1$. That is, there is a branch of non trivial endemic equilibrium points emerging from zero, such that, for every value of R_0 greater 1, there exists a unique non trivial equilibrium.

Analyzing the nullcline (2.10), we can conclude that if infections by additive multiple contacts are not considered ($\phi_j = 0$, for $j = 1, 2, 3, 4, 5, 6$), then model (2.1) presents a unique endemic equilibrium point if and only if $R_0 > 1$. This result is analogous to the principal result shown in [18] in which an unique endemic equilibrium point exists if and only if $R_0 > 1$ for model (2.1). On the other hand, when additive multiple contacts are considered ($\phi_j \neq 0$, for some $j = 1, 2, 3, 4, 5, 6$) other scenario are possible. Particularly, multiple endemic equilibria points can exist when $R_0 < 1$. In other words, when the model considers only infections by single contacts or a fraction of the infections by single contacts, the control strategy of bringing R_0 below 1 is enough to control the disease; in contrast, when the model considers infections not only by single contacts but also infections by additive multiple contacts, the control strategy of bringing $R_0 < 1$ is not enough to control the epidemic outbreak. In this point, we want to underline the difference between the number of new infections according to models (2.1) and (2.1) in [18], a fact that is not properly captured by the fact that both models share the same value of R_0. We can see that R_0 underestimates the real number of new infections in model (2.1) and overestimates the number of new infections in [18].

In the next subsection, we analyze the dynamics of the infectious disease assuming another contagion mechanisms.

2.3. Infections as result of additive multiple contacts: second model

For the second model, we assume that new infections by additive multiple contacts increase as a function of the infectious agents as model (2.1). But, in this case, we also assume that the incidence rate decreases as a function of the infectious sources. One can imagine scenarios in which the saturation effect on the total number of new infections is not a function of each single variable, but a more general one. This is being studied in a separate work.

Here, we propose the model

$$\begin{aligned}
\dot{S} &= \Lambda - \kappa_1 SE - \kappa_2 SI - \kappa_3 SV - \tfrac{F_1(E,I,V)}{H(E,I,V)} S - \mu S,\\
\dot{E} &= \kappa_1 SE + \kappa_2 SI + \kappa_3 SV + \tfrac{F_1(E,I,V)}{H(E,I,V)} S - (\alpha + \mu) E,\\
\dot{I} &= \alpha E - \omega_1 I,\\
\dot{R} &= \gamma I - \mu R,\\
\dot{V} &= \xi_1 E + \xi_2 I - \sigma V.
\end{aligned} \tag{2.14}$$

In model (2.14), expression $F_1(E, I, V)$ is given in (2.2) and

$$H(E, I, V) = a_0 + a_1 E + a_2 I + a_3 V + a_4 E^2 + a_5 I^2 + a_6 V^2 + a_7 EI + a_8 EV + a_9 IV. \tag{2.15}$$

With $a_0 > 0$ and $a_l \geq 0$ for $l = 1, ..., 9$.

The demographic and epidemiological parameters in this model are defined in an analogous way to model (2.1).

For this scenario, we define the infection force by

$$G(E, I, V) = \kappa_1 E + \kappa_2 I + \kappa_3 V + \frac{F_1(E, I, V)}{H(E, I, V)}. \tag{2.16}$$

Then, the number of new infected individuals is given by

$$G(E, I, V)S. \tag{2.17}$$

In model (2.14), the infection rates for the additive multiple contacts are $\frac{\phi_j}{H(E,I,V)}$, for $j = 1, 2, 3, 4, 5, 6$, which are decreasing functions of the infectious agent. Notice that, in this new model, new infected individuals by additive multiple contacts of susceptible individuals with two exposed individuals, two symptomatic ones, and two contaminated surfaces are modeled by $\frac{\phi_1 SE^2}{H(E,I,V)}$, $\frac{\phi_2 SI^2}{H(E,I,V)}$ and $\frac{\phi_3 SV^2}{H(E,I,V)}$, respectively. Also, $\frac{\phi_4 SEI}{H(E,I,V)}$, $\frac{\phi_5 SEV}{H(E,I,V)}$ and $\frac{\phi_6 SIV}{H(E,I,V)}$ describe new infections due to the effective contact of susceptible individuals with two different infectious sources. The main difference between models (2.1) and (2.14) is the fact that the number of new infections by additive multiple contacts is bounded here.

We will show once more that this new model also shares the value of R_0 with Yang's model as well as model (2.1) and model (2.1) simplified.

To wit, the basic reproduction number for model (2.14) is given by

$$R_0 = R_0^E + R_0^I. \tag{2.18}$$

Where R_0^E and R_0^I are the same expressions defined in (2.6).

Notice that once again R_0 is independent of the infection rates associated to infections by additive multiple contacts. We want to explore the consequences of the fact that the basic reproduction number in models (2.1), its simplification, model (2.14) and Yang's model in [18] are the same. Also, the value of R_0 coincides when contagions by additive multiple contacts in model (2.14) are not considered, which will be called model (2.14) simplified. Again, this result is unexpected since every single model describes different contagion mechanisms.

That is, for the four models describing different epidemiological mechanisms, R_0 is the same. The four models mentioned before are listed in the following: model only considering single contacts (model (2.1) and (2.14) with $\phi_j = 0$ for $j = 1, 2, 3, 4, 5, 6$), model only considering single contacts but those contagions decrease when the pathogen agents increase (model (2.1) in [18]), model considering not only infections by single contacts but also contagions by additive multiple contacts which have a unbounded increasing when the pathogen agents increase (model (2.1)) and finally model considering not only infections by single contacts but also contagions by additive multiple contacts which have an bounded increasing when the pathogen agents increase (model (2.14)). Notice that, R_0 underestimates the real number of new infections for models model (2.1) and (2.14) and overestimates the real number of new infections for model (2.1) in [18].

In general, the basic reproduction number is a good descriptor of the number of new infections when the number of new infections corresponds to the mass action law, if this is not the case, R_0 can underestimate or overestimate the actual number of new infections.

Now, we analyze the existence of equilibria points for model (2.14).

2.4. Equilibria solutions for model (2.14)

In this case, the equilibria points, for model (2.14), are given by the intersection points of (2.9) and

$$S_2(I^*) = \frac{(\alpha + \mu)\omega_1}{Y_1 + Y_2 + Y_3}, \tag{2.19}$$

with

$$Y_1 = \kappa_1\omega_1 + \alpha\,\kappa_2 + \frac{\kappa_3\left(\xi_1\omega_1 + \xi_2\alpha\right)}{\sigma}, \tag{2.20}$$

$$Y_2 = \frac{1}{H(E^*, I^*, V^*)}\left(\frac{\phi_1\omega_1^2}{\alpha} + \alpha\phi_2 + \frac{\left(\xi_1\omega_1 + \xi_2\alpha\right)^2\phi_3}{\alpha\sigma^2}\right) I^*, \tag{2.21}$$

and

$$Y_3 = \frac{1}{H(E^*, I^*, V^*)}\left(\phi_4\omega_1 + \frac{\left(\xi_1\omega_1 + \xi_2\alpha\right)}{\sigma}\left(\frac{\omega_1}{\alpha}\phi_5 + \phi_6\right)\right) I^*. \tag{2.22}$$

Notice that $H(E^*, I^*, V^*)$ is a function of the equilibrium for I^*, which is

$$H(E^*, I^*, V^*) = 1 + \left(1 + \frac{\omega_1}{\alpha} + \frac{\omega_1^2}{\alpha^2} + \frac{\xi_1\omega_1 + \xi_2\alpha}{\alpha\sigma}\left(1 + \frac{\omega_1}{\alpha} + \frac{\xi_1\omega_1 + \xi_2\alpha}{\alpha\sigma}\right)\right)(I^*)^2 . \tag{2.23}$$

Observe that if $\phi_j = 0$ for $j = 1, 2, 3, 4, 5, 6$, $S_2(I^*)$ is a constant function.
The nullclines of model (2.14) satisfy $S_1(0) = \frac{\Lambda}{\mu} \equiv S_0$, $S_1\left(\frac{\Lambda\,\alpha}{\omega_1(\alpha+\mu)}\right) = 0$, $S_2(0) = \frac{S_0}{R_0}$, $\lim\limits_{I^*\to\infty} S_2(I^*) = \frac{S_0}{R_0}$ and $\frac{dS_2(0)}{dI^*} = -\frac{(\alpha+\mu)\omega_1\left(\frac{\phi_1{\omega_1}^2}{\alpha} + \alpha\,\phi_2 + \frac{(\xi_1\omega_1+\xi_2\alpha)^2\phi_3}{\alpha\,\sigma^2} + \phi_4\omega_1 + \frac{(\xi_1\omega_1+\xi_2\alpha)(\omega_1\phi_5+\phi_6\alpha)}{\alpha\,\sigma}\right)}{\left(\kappa_1\omega_1 + \alpha\,\kappa_2 + \frac{(\xi_1\omega_1+\xi_2\alpha)\kappa_3}{\sigma}\right)^2}$.

In the following, we prove a result on existence of nontrivial equilibria points.

Theorem 2.3. *For model (2.14).*
Let $\Omega = \frac{\mu\left(\frac{\phi_1{\omega_1}^2}{\alpha} + \alpha\,\phi_2 + \frac{(\xi_1\omega_1+\xi_2\alpha)^2\phi_3}{\alpha\,\sigma^2} + \phi_4\omega_1 + \frac{(\xi_1\omega_1+\xi_2\alpha)(\omega_1\phi_5+\phi_6\alpha)}{\alpha\,\sigma}\right)}{\left(\kappa_1\omega_1 + \alpha\,\kappa_2 + \frac{(\xi_1\omega_1+\xi_2\alpha)\kappa_3}{\sigma}\right)^2}$ *and* $R_0 = \frac{\kappa_1}{\alpha+\mu}S_0 + \frac{\kappa_2\alpha}{\omega_1(\alpha+\mu)}S_0 + \frac{\kappa_3(\xi_1\omega_1+\xi_2\alpha)}{\sigma\omega_1(\alpha+\mu)}S_0$.

a) If $\Omega > 1$ *and* $R_0 < 1$, *then there are at least two non trivial endemic equilibrium points.*
b) If $\Omega > 1$ *and* $R_0 > 1$, *then there is one non trivial endemic equilibrium point.*

Proof. In case a), for values of R_0 close to one, $S_2(I^*)$ crosses $S_1(I^*)$, with negative derivative, in $I^* = 0$. In such case, there are values of I^* with $S_2(I^*) < S_1(I^*)$. Since $S_1(I)$ has negative derivative for all I^*, it follows $S_1(0) = S_0 > S_1(I^*)$ for all I^*. As $\lim\limits_{I^*\to\infty} S_2(I^*) = \frac{S_0}{R_0}$, and by hypothesis $R_0 < 1$, we conclude that there are values of I^* such that $S_2(I^*) > S_1(I^*)$. By the continuity if I^* goes to infinity, at least two non trivial equilibrium point exists if I^* goes to infinity. In particular, there is a certain value of R_0, which we will call R_0^* in which $S_2(I^*)$ touches $S_1(I^*)$ tangentially in I_c^*. After that, the tangential point I_c^* bifurcates in two points that are intersection points of $S_1(I^*)$ and $S_2(I^*)$, which are denoted by I_I^* and I_2^*.
On the other hand in case b), if $R_0 > 1$, then $S_2(0) < S_1(0)$ and, by the continuity of $S_2(I^*)$ when $I^* \to \infty$ there is at least one non trivial endemic equilibrium. □

Option a) in Theorem 2.3 corresponds to option c) in Theorem 2.1 which indicates also the possibility of a backward bifurcation in model (2.14). Both scenarios would require additional control measures for eradicating the epidemic, even after bringing R_0 below 1.

Notice that if contagions by additive multiple contacts are not considered, the nullcline S_2 is a constant function. In this case, there is a unique endemic equilibria point if and only if $R_0 > 1$. This result coincides with the result shown in [18] in which model (2.1) presents a unique endemic equilibrium point if and only if $R_0 > 1$. However, we prove that when contagions by additive multiple contacts are considered, non trivial equilibria can exist when $R_0 < 1$.

Therefore, we have shown that the dynamics of the disease can change when contagions by additive multiple contacts are considered and some conditions over the parameters of model (2.14) are satisfied. Particularly, we can obtain an analogous conclusion to the conclusion for model (2.1). When the model considers only contagions by single contacts or a fraction of them, the control strategy of bringing R_0 below 1 is enough to control the epidemic outbreak; in contrast, when the model considers contagions not only by single contacts but also by additive multiple contacts, the control strategy of bringing R_0 below 1 is not enough to control the infectious disease.

In the following section, we estimate some values of the parameters of the models proposed.

3. Parameter estimates

In this section, parameters related to the transmission and shedding rates are estimated to fit the solutions of models (2.1) and (2.14) to the cumulative cases of confirmed infected individual in Mexico for COVID-19

TABLE 1. Values of some epidemiological parameters for models (2.1) and (2.14).

Parameter	Value	Units	Source
Λ	5661.198270	Day^{-1}	[26]
μ	4.43×10^{-5}	Day^{-1}	[26]
$\frac{1}{\alpha}$	3.03	Day^{-1}	[27]
ω	1.7826×10^{-5}	Day^{-1}	[28]
$\frac{1}{\gamma}$	5	Day^{-1}	[27]
σ	1	Day^{-1}	[18]

[23]. We also estimate the transmission and shedding rates when the contagions by additive multiple contacts are not considered ($\phi_j = 0$ for $j = 1, 2, 3, 4, 5, 6$) using the cumulative cases of infected individuals in Mexico. The data used represents the confirmed cases of COVID-19 in Mexico from March 4th, 2020 to October 11th, 2020 date in which the first wave approximately ended.

The following values were taken as initial conditions: $S_0 = 127\ 792\ 286$ for the total Mexican population, $I_0 = 10$ the number of confirmed cases in the data. We also assumed that the number of exposed individuals, recovered individuals and virus at the beginning of the infection are given by $10, 10$ and 100, respectively.

To calibrate these models, the unknown parameters

$$\phi = (\kappa_1, \kappa_2, \kappa_3, \phi_1, \phi_2, \phi_3, \phi_4, \phi_5, \phi_6, \xi_1, \xi_2, \theta)$$

are estimated using a Bayesian approach based on MCMC (Markov Chain Monte Carlo). This estimation uses the pytwalk implementation on Python [24], considering some parameter values that appear in the epidemiological literature related to generation intervals of COVID-19 (see Tab. 1). To see more about generation times in epidemic models see [25].

It is assumed that data $y = (y_0, y_1, ..., y_n)$ consisting of the cumulative daily cases of infected individuals can be modeled by

$$y_t = C(t; \eta) + \eta_t, \tag{3.1}$$

where $t = 0, ..., n$, and η_t are independent identically distributed random variables with normal distribution with mean 0 and unknown θ^2 variance.

$$C(t; \eta) \quad = \quad \sum_{i=0}^{t} I(i; \eta) \quad = \quad y_0 + \sum_{i=1}^{t} I(i; \eta), \tag{3.2}$$

where $I(i; \eta)$ is the solution of the ODE's system (2.1) and system (2.14) for the I compartment, given a fixed vector of parameters η with initial values $(S_0, E_0, I_0, R_0, V_0)$. This means, $I(i; \eta)$ are the infected individuals at time i given η.

The prior distribution for the unknown parameters assumes independence among them. We propose different Gamma distributions for the infection and the shedding rates; see (3.4). To take into account the possible asymmetry of the parameter distribution and plausible values concentrated towards zero, we propose gamma distributions for the parameters κ_1, κ_2, κ_3, ϕ_1, ϕ_2, ϕ_3, ϕ_4, ϕ_5, ϕ_6, ξ_1, ξ_2 with expected values in agreement with the results presented in [18, 29], allowing the parameters to take values in all positive real numbers. We also consider different orders of magnitude for the parameters κ_1, κ_2, κ_3, ϕ_1, ϕ_2, ϕ_3, ϕ_4, ϕ_5, and ϕ_6, and the parameters ξ_1 and ξ_2. Therefore:

$$\pi(\eta, \theta^2) = \Pi_1(\kappa)\Pi_2(\phi)\Pi_3(\xi)\pi_{12}(\theta^2) \tag{3.3}$$

with $\Pi_1(\kappa) = \pi_1(\kappa_1)\pi_2(\kappa_2)\pi_3(\kappa_3)$, $\Pi_2(\phi) = \pi_4(\phi_1)\pi_5(\phi_2)\pi_6(\phi_3)\pi_7(\phi_4)\pi_8(\phi_5)\pi_9(\phi_6)$ and $\Pi_3(\xi) = \pi_{10}(\xi_1)\pi_{11}(\xi_2)$.

Where

$$\begin{aligned} \kappa_1 &\sim \Gamma(1, 10^{10}), & \phi_4 &\sim \Gamma(1, 10^{55}), \\ \kappa_2 &\sim \Gamma(1, 10^{10}), & \phi_5 &\sim \Gamma(1, 10^{55}), \\ \kappa_3 &\sim \Gamma(1, 10^{10}), & \phi_6 &\sim \Gamma(1, 10^{55}), \\ \phi_1 &\sim \Gamma(1, 10^{55}), & \xi_1 &\sim \Gamma(1, 10^{5}), \\ \phi_2 &\sim \Gamma(1, 10^{55}), & \xi_2 &\sim \Gamma(1, 10^{5}), \\ \phi_3 &\sim \Gamma(1, 10^{55}), & \theta &\sim \Gamma(1, 10^{2}). \end{aligned} \tag{3.4}$$

With the two parameters β and δ inside the parentheses representing a gamma distribution with shape parameter β and inverse scale parameter δ. Notice that $z \sim \Gamma(\beta, \delta)$ means $E(z) = \frac{\beta}{\delta}$ and $Var(z) = \frac{\beta}{\delta^2}$.

The pytwalk based on MCMC was simulated in Python for 70 000 samples with 35 000 burnin. Table 2 shows the maximum *a posteriori* estimators, (MAP), the posterior mean and the credible intervals, which were calculated with the library ArviZ, for models (2.1) and (2.14) and the corresponding simplified models with $\phi_j = 0$ for $j = 1, 2, 3, 4, 5, 6$.

4. Numerical simulations

In this section, we show numerical simulations of the solutions of models (2.1), (2.14) and their simplifications for the exposed and infectious individuals. We use the values estimated for the transmission and shedding rates that were calculated using the methodology presented in the above section and the values of the parameters given in Tables 1 and 2.

In the following, we show that fitting models (2.1) and (2.14) to the data produce different results. Model (2.1) shows a forward bifurcation, while model (2.14) shows evidence of a backward bifurcation, as described in the following paragraphs.

For model (2.1), using the MAP estimated parameters given in Table 2, $\frac{\delta_2 \alpha^2 \mu \sigma^2}{\delta_3{}^2} = 0.00083 < 1$. Therefore, the condition of Theorem 2.2 is satisfied. Then, model (2.1) exhibits a forward bifurcation at E_0 when $R_0 = 1$. That is, a locally asymptotically stable non trivial equilibrium, E_1, emerges from the disease-free equilibrium E_0. For these values of the parameters $R_0 = 1.07443546$ and the equilibria points are $E_0 = (1.277922860 \times 10^8, 0, 0, 0, 0)$, which is unstable, and $E_1 = (1.1909 \times 10^8, 1167.6234, 1925.9804, 8.6952 \times 10^6, 9.5332 \times 10^{-7})$. The eigenvalues associated with E_1 are $\lambda_1 = -1.0000002$, $\lambda_2 = -0.5301130$, $\lambda_3 = -0.0000443$ and $\lambda_{4,5} = -0.0000196 \pm 0.0006343i$. In this scenario, the classical policy of bringing R_0 below one is enough to control the infectious disease.

Figure 1 shows numerical simulations associated to model (2.1) with the values estimated of the parameters given in Table 2. Figure 1 case (a) shows the recorded number of cumulative infectious individuals in Mexico and the solution $I(t)$ for model (2.1) using the MAP and MEAN estimated parameters. Using the MAP estimated parameters, Figure 1 cases (b) and (c) show the asymptotic mathematical behavior for long time of the exposed and infectious individuals when the susceptible population varies, respectively.

For model (2.14), when the MAP estimated parameters are used, $\Omega = 9.0371 \times 10^6 > 1$ and $R_0 = 1.0570 > 1$. Then, the conditions in Theorem 2.3 case b) are satisfied. Therefore, there is one non trivial endemic equilibrium. In this scenario, the equilibrium points are $E_0 = (1.277922860 \times 10^8, 0, 0, 0, 0)$, which is unstable, and $E_1 = (1.1767 \times 10^8, 1358.8864, 2241.4662, 1.0119 \times 10^7, 0.0001)$. The eigenvalues associated to E_1 are $\lambda_1 = -1.0000017$, $\lambda_2 = -0.4551649$, $\lambda_3 = -0.0034073$, $\lambda_4 = -0.0002087$, and $\lambda_5 = -0.0000443$. Therefore, E_1

TABLE 2. Estimated values of infectious and shedding rates for models (2.1), (2.14) and their simplifications with their credible intervals.

Model (2.1)	MAP estimate	Posterior mean	95% credible interval
κ_1	3.63×10^{-15}	5.43×10^{-16}	$(3.08 \times 10^{-18}, 2.13 \times 10^{-15})$
κ_2	1.68×10^{-09}	1.70×10^{-9}	$(1.65 \times 10^{-9}, 1.79 \times 10^{-9})$
κ_3	4.69×10^{-09}	3.14×10^{-9}	$(4.91 \times 10^{-10}, 4.97 \times 10^{-9})$
ϕ_1	2.95×10^{-25}	1.98×10^{-25}	$(3.52 \times 10^{-26}, 3.49 \times 10^{-25})$
ϕ_2	4.98×10^{-17}	5.20×10^{-17}	$(1.47 \times 10^{-19}, 1.50 \times 10^{-16})$
ϕ_3	2.03×10^{-10}	3.23×10^{-10}	$(6.05 \times 10^{-11}, 8.36 \times 10^{-10})$
ϕ_4	6.52×10^{-22}	2.55×10^{-21}	$(3.75 \times 10^{-24}, 5.47 \times 10^{-21})$
ϕ_5	9.35×10^{-09}	9.07×10^{-9}	$(7.52 \times 10^{-9}, 9.85 \times 10^{-9})$
ϕ_6	3.93×10^{-23}	1.17×10^{-23}	$(8.39 \times 10^{-25}, 3.93 \times 10^{-23})$
ξ_1	2.21×10^{-10}	2.51×10^{-10}	$(1.10 \times 10^{-11}, 4.97 \times 10^{-1})$
ξ_2	3.61×10^{-10}	2.61×10^{-10}	$(3.73 \times 10^{-11}, 3.98 \times 10^{-10})$
R_0	1.07443546	1.085077057	(1.052769066, 1.145820736)
R_0^I	1.074434052	1.085076846	(1.052769064, 1.145820735)
R_0^E	1.41×10^{-6}	2.11×10^{-7}	(1.141887162, 1.142011629)
Model (2.14)	**MAP estimate**	**Posterior mean**	**95% credible interval**
κ_1	6.08×10^{-10}	4.97×10^{-10}	$(4.23 \times 10^{-10}, 6.08 \times 10^{-10})$
κ_2	1.29×10^{-09}	1.37×10^{-9}	$(1.29 \times 10^{-9}, 1.42 \times 10^{-9})$
κ_3	1.00×10^{-07}	9.99×10^{-8}	$(9.94 \times 10^{-8}, 1.00 \times 10^{-7})$
ϕ_1	1.00×10^{-07}	9.99×10^{-8}	$(9.97 \times 10^{-8}, 1.00 \times 10^{-7})$
ϕ_2	9.96×10^{-07}	9.99×10^{-8}	$(9.96 \times 10^{-8}, 1.00 \times 10^{-7})$
ϕ_3	7.99×10^{-08}	8.86×10^{-8}	$(7.32 \times 10^{-8}, 9.96 \times 10^{-8})$
ϕ_4	6.49×10^{-08}	3.80×10^{-8}	$(4.40 \times 10^{-9}, 7.99 \times 10^{-8})$
ϕ_5	9.71×10^{-08}	9.33×10^{-8}	$(6.49 \times 10^{-8}, 9.98 \times 10^{-8})$
ϕ_6	9.73×10^{-09}	6.90×10^{-9}	$(2.31 \times 10^{-9}, 9.71 \times 10^{-9})$
ξ_1	3.13×10^{-08}	4.39×10^{-7}	$(2.39 \times 10^{-8}, 1.53 \times 10^{-6})$
ξ_2	3.61×10^{-10}	2.53×10^{-7}	$(3.13 \times 10^{-10}, 1.60 \times 10^{-6})$
R_0	1.05704008	1.064870791	(1.057040085, 1.070802257)
R_0^I	0.82153743	0.872401958	(0.82153743, 0.90643969)
R_0^E	0.235502655	0.192468832	(0.163765045, 0.235522764)
Simplified Model	**MAP estimate**	**Posterior mean**	**95% credible interval**
κ_1	2.67×10^{-9}	2.67×10^{-9}	$(2.66 \times 10^{-9}, 2.67 \times 10^{-9})$
κ_2	4.65×10^{-15}	1.23×10^{-12}	$(3.07 \times 10^{-15}, 4.27 \times 10^{-12})$
κ_3	1.00×10^{-6}	1.00×10^{-6}	$(1.00 \times 10^{-6}, 1.00 \times 10^{-6})$
ξ_1	1.19×10^{-8}	4.52×10^{-7}	$(1.19 \times 10^{-8}, 8.60 \times 10^{-87})$
ξ_2	4.48×10^{-9}	2.7×10^{-7}	$(4.48 \times 10^{-9}, 8.94 \times 10^{-7})$
R_0	1.034679482	1.034772627	(1.034669464, 1.035017591)
R_0^I	5.83×10^{-6}	0.000964435	$(5.58 \times 10^{-6}, 0.003298038)$
R_0^E	1.034673647	1.033808192	(1.031697278, 1.034667182)

is a locally asymptotically stable equilibrium. However, E_1 does not emerge from the disease-free equilibrium. Therefore, the infectious disease may not be eradicated even though if $R_0 < 1$. Figure 1 case (d) shows the recorded number of cumulative infectious individuals in Mexico and the solution $I(t)$ for model (2.14) using the MAP and MEAN estimated parameters. For the MAP estimated parameters, Figure 1 cases (e) and (f) show the asymptotic dynamics of the exposed and infectious individuals as a function of the susceptible population, respectively.

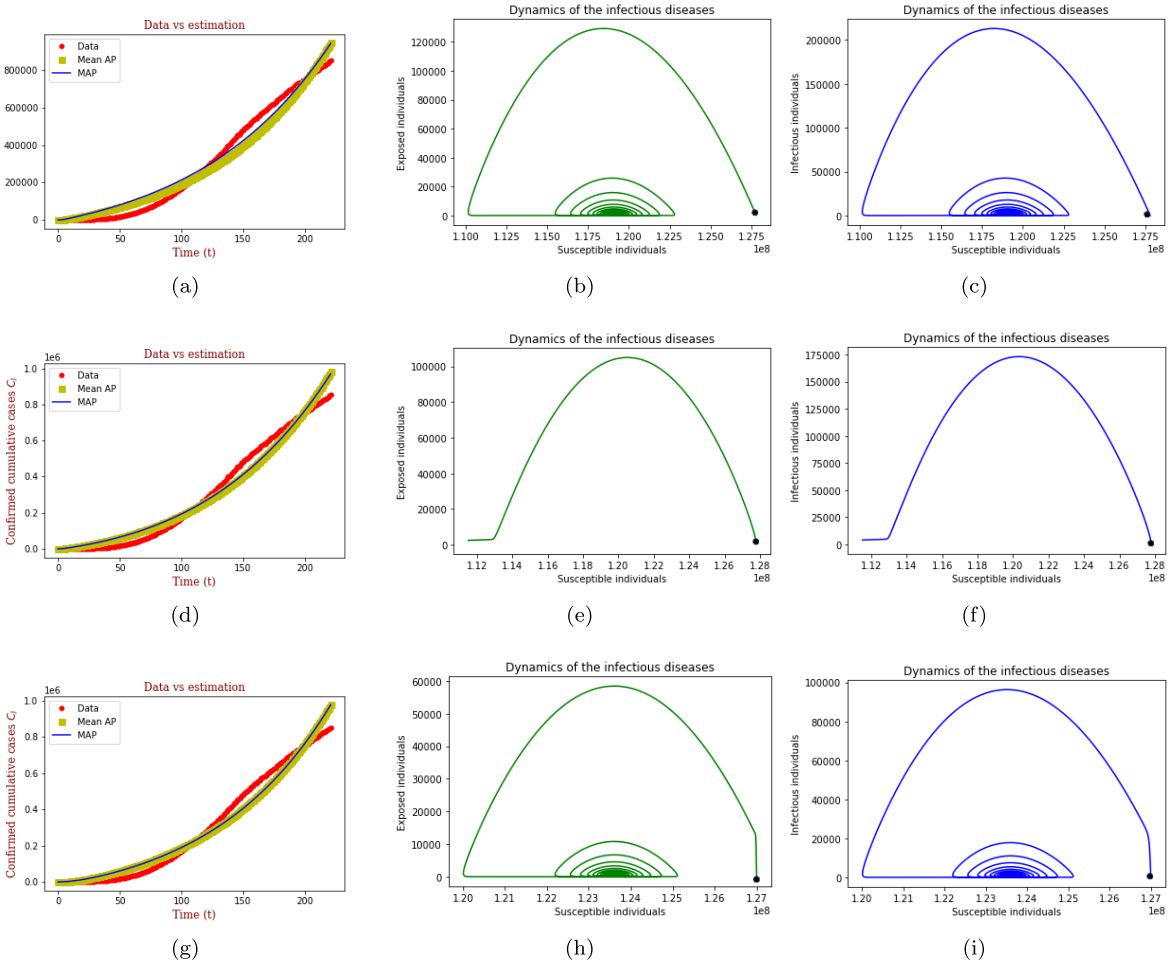

FIGURE 1. Cases (a), (d) and (g) show the recorded number of cumulative infectious individuals in Mexico from March 04 to October 11, 2020 with the solution $I(t)$ for models (2.1), (2.14) and the simplified model, respectively. Other cases in Figure 1 show the phase portraits associated to these model in which the asymptotic dynamics of the exposed, infectious and susceptible individuals are shown. Observe that the phase portraits associated to models (2.1) (cases (b) and (c)) and the simplified model (cases (e) and (f)) show that the solutions present an oscillatory behavior. In contrast, the phase portrait associated to model (2.14) (cases (h) and (i)) shows that the solutions have a monotone behavior. For the numerical simulations, the initial condition $(1.277922860 \times 10^8, 10, 10, 10, 100)$ is marked by a point.

Now, we illustrate the case in which the additive multiple contacts are not considered ($\phi_j = 0$ for $j = 1, 2, 3, 4, 5, 6$ in models (2.1) and (2.14)). With the MAP estimated values of the parameters given in Table 2, $R_0 = 1.0347$ and $E_1 = (1.2361 \times 108, 561.2509, 925.7763, 4.1796 \times 10^6, 0.00001)$. The eigenvalues for E_1 are $\lambda_1 = -1.0000012$, $\lambda_2 = -0.2000642$, $\lambda_3 = -0.0000443$, $\lambda_{4,5} = -0.0000229 \pm 0.0007029i$. Therefore, E_1 is a locally asymptotically stable equilibrium. Numerical simulations associated to this scenario are shown in Figure 1. In case (g), it is shown the cumulative infectious individuals in Mexico and the solution $I(t)$ for these models when the MAP and MEAN estimated parameters are used. In cases (h) and (i), it is shown the phase portrait of solutions of the model for the exposed and infectious individuals as a function of the susceptible individuals, respectively.

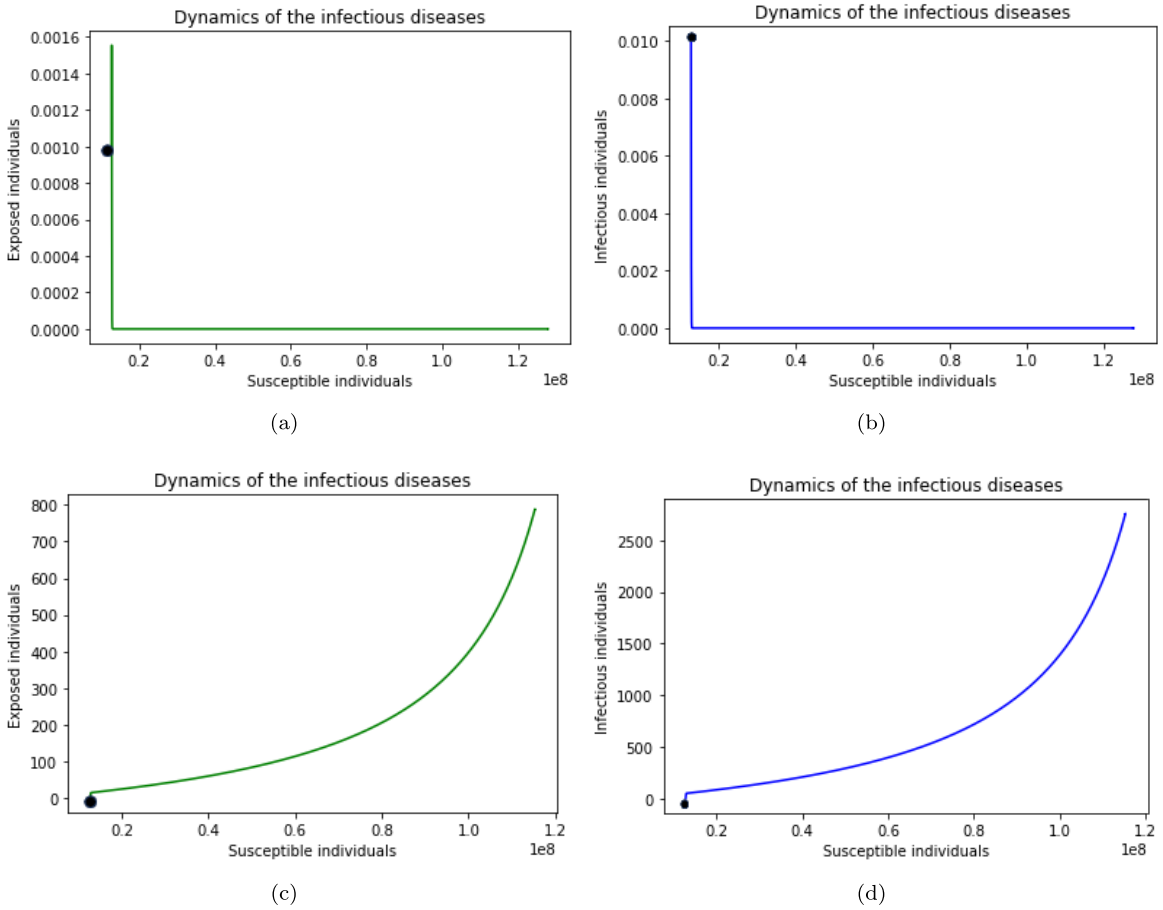

FIGURE 2. Depending on the initial conditions, the exposed and infectious individuals go to different equilibrium points. Cases (a) and (b) show that solutions go to the disease-free equilibrium, E_0 for the initial condition $(1.277922860 \times 10^8, 0.001, 0.01, 0.001, 0.0001)$. In contrast, cases (c) and (d) show that exposed and infectious individuals go to the endemic equilibrium E_2 for the initial condition $(1.277922860 \times 10^8, 1, 1, 1, 1)$. The initial condition is marked by a point.

In the following, a relevant scenario, from an epidemiological point of view, will be shown. Observe that, model (2.14) with the MAP values of Table 2 satisfies the condition $\Omega = 9.0371 \times 10^6 > 1$ in Theorem 2.3. If R_0 decreases below 1, multiple endemic equilibria exists since conditions in Theorem 2.3 for case (a) are satisfied. To exemplify this case, it is considered $\alpha = 0.7$. In this scenario, $R_0 = 0.9349$. Therefore, $E_0 = (1.277922860 \times 10^8, 0, 0, 0, 0)$ is a locally asymptotically stable equilibrium. Also, $E_1 = (1.2779 \times 10^8, 0.00002, 0.00008, 0.4497, 9.2610 \times 10^{-13})$ is a unstable equilibrium since E_1 has the eigenvalues $\lambda_1 = -1.0000019$, $\lambda_2 = -0.8318070$, $\lambda_3 = 0.01095240$, $\lambda_4 = -0.0000002$, $\lambda_5 = -0.0000886$. In contrast, $E_2 = (1.1533 \times 10^8, 788.4764, 2758.8103, 1.2455 \times 10^7, 0.000026)$ is a locally asymptotically stable equilibrium since it has associated the eigenvalues $\lambda_1 = -1.0000018$, $\lambda_2 = -0.8360078$, $\lambda_3 = -0.0261344$, $\lambda_4 = -0.0000750$, $\lambda_5 = -0.0000443$. Therefore, in this scenario, model (2.14) shows a bistability phenomenon between E_0 and E_2 when $R_0 < 1$. Therefore, an epidemic outbreak can occur even though $R_0 < 1$ if the initial conditions belong to the basins of attraction of the endemic equilibrium E_2. Figure 2 cases (a) and (b) show that the exposed and infectious individuals go to the disease-free equilibrium E_0 when the initial conditions are $S_0 = 127\ 792\ 286$,

$E_0 = 0.001$, $I_0 = 0.01$, $R_0 = 0.001$ and $V_0 = 0.0001$. In contrast, Figure 2 cases (c) and (d) show that the exposed and infectious populations go to the endemic equilibrium E_2, for the initial condition $S_0 = 127\ 792\ 000$, $E_0 = 1$, $I_0 = 1$, $R_0 =$ and $V_0 = 1$, even though $R_0 < 1$. In this scenario, a bistability phenomenon occurs between the disease-free equilibrium and an endemic equilibrium when $R_0 < 1$.

It is worthwhile noticing that in general not including additive multiple contacts underestimates the value of R_0, potentially turning control measures uneffective. To wit, by comparing the value of R_0 for each case mentioned above we can conclude that the value of R_0 for model describing only contagions by single contacts ($R_0 = 1.0347$) is smaller than the value of R_0 for model describing both types of contagions: contagions by single contacts and a bounded number of contagions by additive multiple contacts ($R_0 = 1.0570$); and contagions by single contacts and an unbounded number of contagions by additive multiple contacts ($R_0 = 1.0744$).

Notice that, even though the value of R_0 is close to one in the last two cases, bringing R_0 below one can not be enough to control the epidemic outbreak. Another potential problem is that even when the value of R_0 is close to one, that is the case in which only contagion by single contacts are considered, such R_0 might be underestimating the number of the secondary infections.

5. Discussion

In epidemiological modeling, the function used to model the force of infection (also called the incidence rate) plays a key role. This function depends on both the susceptible and infectious classes, say, $f(S, I)$. The function used as the force of infection must describe the mechanisms of transmission of the disease. It such a function can be written in a Taylor's series form, $f(S, I) = a_0 + a_1 S + a_2 I + a_3 SI + a_4 S^2 + a_5 I^2 + ...+$ where the values of $a_i \in \mathbb{R}$, for $i \in \mathbb{N}$, depend on the epidemiological mechanism being modeled. The most common function used to describe the force of infection is $f(S, I) = \beta SI$, the familiar mass action law, which is obtained when $a_i = 0$, for $i \neq 3$, and $a_3 = \beta$ is defined as the infection rate. However, the choice of this function neglects the fact that the mass action law only models infections by which the minimum infectious load is reached by one single contact. As we have shown, the mass action law does not model infections by additive multiple contacts nor those influenced by saturation processes [28, 30, 31], among others. This fact has relevant consequences for the application of control policies. We should beware of these shortcomings when using R_0 as the only element to determine control strategies in models in which the force of infection includes nonlinear terms like a generalized mass action law.

The basic reproduction number, R_0 is widely used to analyze the dynamics of infectious diseases. As a general definition, R_0 is the average number of secondary infections produced by a single infectious individual during its infectious period in a completely susceptible population. From this definition, it is clear that when $R_0 < 1$, the infection will be cleared from the population. In contrast, when $R_0 > 1$, there will be an epidemic outbreak. Also, in an endemic infection, R_0 might be used in two ways: to measure the intensity of the infection and to determine which control measures and what magnitude should be chosen to bringing R_0 below one. Therefore, it is important to acknowledge the phenomena that are not captured by R_0, and avoiding the use of R_0 for making decisions when those phenomena occur.

A key feature of additive multiple contacts is the fact that being a high order process, they are not captured by R_0. We show that when two models differ only in a term describing additive multiple contacts, they will have the same R_0, even though the real number of secondary infections might be different. In such a situation, the threshold property of R_0 might fail since for $R_0 < 1$, an epidemic outbreak might occur. In this scenario, an endemic equilibrium exists for values of $R_0 < 1$. In such a scenario, in an endemic infection, $R_0 > 1$ is not a good measure of the intensity of the infection for values of R_0 close to one. We also show that saturation phenomena are not captured by R_0, then, if we derive our public health control strategies from epidemiological models and carry on any mistakes reflected in the value of R_0, we might miss the mark. Therefore, if infections by additive multiple contacts or any saturation effects in the mass action law are neglected in the modeling process, R_0 could be the same, but the corresponding control interventions could be unsufficient or wasteful. In contrast, we want to point out that when the new infections occur by one single contact and saturation phenomena do not occur, modelling the force of infection by the mass action law, $f(S, I) = \beta SI$, is the better choice since, in this

case, the basic reproduction number functions as a threshold parameter through an epidemic outbreak can be controlled and it is useful to determine control strategies and in which magnitude they should be implemented.

Assuming that the viral load necessary for a new infection to occur is only reached by a single contact might in some cases be too restrictive. It might be even worse, when modeling new infections using only the mass action law, infections due to additive multiple contacts are neglected, but required, we have already established that they can be relevant in the evolution of an epidemic.

In the particular examples shown in this work, we emphasized the importance of not neglecting contagions by additive multiple contacts, which for COVID-19 are not only possible but likely very common because susceptible individuals are repeatedly in contact with infectious sources and individuals. Recent epidemiological research has shown that asymptomatic individuals and mild symptomatic ones have similar viral load while individuals with severe infection have viral load up to 60 times higher than individuals with mild infection [32–34]. It is not unrealistic to assume that simultaneous contribution of free viruses in the environment by infectious and exposed individuals is enough for contagions by additive multiple contacts to happen. Even if those sources supply a low viral load, additive multiple contacts could still provide the minimum viral load needed to cause a new infection. Particularly, Meyerowitz *et al.* (2020) suggest that infections by contaminated surfaces are possible albeit in small numbers [35]. Notice that the analysis of the different models shows that the results still apply even if infections by contaminated environments are not considered.

As noted by previous works ([36] in the case of over spreading), when considering R_0 as the principal element for the design of control policies, one should also pay attention to possible underestimation or overestimation of the real number of secondary infections. Nonlinear phenomena affecting infections won't be properly captured by R_0, potentially leading to insufficient or wasteful campaigns [37].

References

[1] K.S. Crump, D.G. Hoel, C.H. Langley and R. Peto, Fundamental carcinogenic processes and their implications for low dose risk assessment. *Cancer Res.* **39** (1976) 2973–2979.

[2] D.L. Sewell, Laboratory-associated infections and biosafety. *Clin. Microbiol. Rev.* **8** (1995) 389–405.

[3] S. Karimzadeh, R. Bhopal and H. Nguyen Tien, Review of infective dose, routes of transmission and outcome of COVID-19 caused by the SARS-COV-2: comparison with other respiratory viruses. *Epidemiol. Infect.* **149** (2021) 1–8.

[4] S. Basu, Close-range exposure to a COVID-19 carrier: transmission trends in the respiratory tract and estimation of infectious dose. medRxiv (2020).

[5] S. Yezli and J.A. Otter,Minimum infective dose of the major human respiratory and enteric viruses transmitted through food and the environment. *Food Environ. Virol.* **3** (2011) 1–30.

[6] G. Bagheri, B. Rhiede, B. Hejazi, O. Schlenczek and E. Bodenschatz, An upper bound on one-to-one exposure to infectious human respiratory particles. *PNAS* **118** (2021) e2110117118.

[7] Wm. Liu, S.A. Levin and Y. Iwasa, Influence of nonlinear incidence rates upon the behavior of SIRS epidemiological models *J. Math. Biol.* **23** (1986) 187–204.

[8] P. van den Driessche and J. Watmough, A simple SIS epidemic model with a backward bifurcation. *J. Math. Biol.* **40** (2000) 525–540.

[9] B. Buonomo and D. Lacitignola, Forces of infection allowing for backward bifurcation in an epidemic model with vaccination and treatment. *Acta Appl Math.* **122** (2012) 283–293.

[10] B. Buonomo and D. Lacitignola, On the dynamics of an SEIR epidemic model with a convex incidence rate. *Ricerche mat.* **57** (2008) 261–281.

[11] V. Capasso and G. Serio, A generalization of the Kermack–McKendrick deterministic epidemic model. *Math. Biosci.* **42** (1978) 41–61.

[12] C. Paulo, M. Correira-Neves, T. Domingos, A.G. Murta and J. Pedrosa, Influenza infectious dose may explain the high mortality of the second and third wave of 1918–1919 influenza pandemic. *PLos One* **5** (2010) e11655.

[13] C.M. Kribs-Zaleta and J.X. Velasco-Hernandez, A simple vaccination model with multiple endemic states. *Math. Biosci.* **164** (2000) 183–201.

[14] A. Tang, Z.D. Tong, H.L. Wang, Y.X. Dai, K.F. Li, J.N. Liu, W.J. Wu, C. Yuan, M.L. Yu, P. Li and J.B. Yan, Detection of novel coronavirus by RT_PCR in stool specimen from asymptomatic child, China. *Emerg. Infect. Dis.* **26** (2020) 1337–1339.

[15] Z. Hu, C. Song, C. Xu, G. Jin, Y. Chen, X. Xu, H. Ma, W. Chen, Y. Lin, Y. Zheng, J. Wang, Z. Hu, Y. Yi and H. Shen, Clinical characteristics of 24 asymptomatic infections with COVID-19 screened among close contacts in Nanjing, China. *Sci. China Life Sci.* **63** (2020) 706–711.

[16] J. Zhou, Y. Tan, D. Li, X. He, T. Yuan and Y. Long, Observation and analysis of 26 cases of asymptomatic SARS-COV2 infection. *J. Infect.* **81** (2020) e69–e70.
[17] J. Cai, W. Sun, J. Huang, M. Gamber, J. Wu and G. He, Indirect virus transmission in cluster of COVID-19 cases, Wenzhou, China, 2020. *Emerg. Infect. Dis.* **26** (2020) 1343–1345.
[18] C. Yang and J. Wang, A mathematical model for the novel coronavirus epidemic in Wuhan, China. *Math. Biosci. Eng.* **17** (2020) 2708–2724.
[19] Y. Jin, W. Wang and S. Xiao, A SIRS model with a nonlinear incidence. *Chaos Solitons Fractals* **34** (2007) 1482–1497.
[20] P. van den Driessche and J. Watmough, Epidemic solutions and endemic catastrophies, in Dynamical Systems and Their Applications in Biology, Vol. 36. American Mathematical Society, Providence (2003) 247–257.
[21] O. Diekmann, J.A.P. Heesterbeek and J.A. Metz, On the definition and the computation of the basic reproduction ratio R_0 in models for infectious diseases in heterogeneous populations. *J. Math. Biol.* **28(4)** (1990) 365–382.
[22] P. Van den Driessche and J. Watmough, Reproduction numbers and sub-threshold endemic equilibria for compartmental models of disease transmission. *Math. Biosci.* **180** (2002) 29–48.
[23] Ministry of Health, Mexico, http://datosabiertos.salud.gob.mx/gobmx/salud/datos_abiertos/datos_abiertos_covid19.zip.
[24] J.A. Christen and C. Fox, A general purpose sampling algorithm for continuous distribution (the t-walk). *Bayesian Anal.* **5** (2010) 263–281.
[25] A. Svensson, A note on generation times in epidemic models. *Math. Biosci.* **208** (2007) 300–3011.
[26] CONAPO, http://www.conapo.gob.mx/work/models/CONAPO/Mapa_Ind_Dem18/index_2.html.
[27] I.G. Violaris, T. Lampros, K. Kalafatakis, G. Ntritsos, K. Kostikas, N. Giannakeas, M. Tsipouras, E. Glavas, D. Tsalikakis and A. Tzallas, Modelling the COVID-19 pandemic: focusing on the case of Greece. *Epidemics* **44** (2023) 100706.
[28] F. Saldaña, H. Flores-Arguedas, A. Camacho and I. Barradas, Modeling the transmission dynamics and the impact of the control interventions for the COVID-19 epidemic outbreak. *Math. Biosci. Eng.* **17** (2020) 4165–4183.
[29] B. Tang, X. Wang, Q. Li, N.L. Bragazzi, S. Tang, Y. Xiao and J. Wu, Estimation of the transmission risk of the 2019-nCoV and its implication for public health interventions. *J. Clin. Med.* **9** (2020) 32046137.
[30] A. Acuña-Zegarra, M. Santana-Cibrian and J.X. Velasco-Hernández, Modeling behavioral change and COVID-19 containment in México: a trade-of between lockdown and compliance. *Math. Biosci.* **325** (2020) 108370.
[31] E.A. Iboi, O. Sharomi, C.N. Ngonghala and A. Gumel, Mathematical modeling and analysis of COVID-19 pandemic in Nigeria. *Math. Biosci. Eng.* **17** (2020) 7192–7220.
[32] Y. Liu, L.M. Yan, L. Wan, T.X. Xiang, A. Le, J.M. Liu, M. Peiris, L.L.M. Poon and W. Zhang, Viral dynamics in mild and severe cases of COVID-19. *Lancet* **20** (2020) 656–657.
[33] L. Zou, F. Ruan, M. Huang, L. Liang, H. Huang, Z. Hong, J. Yu, M. Kang, Y. Song, J. Xia, Q. Guo, T. Song, J. He, H.L. Yen, M. Peiris and J. Wu, SARS-CoV-2 viral load in upper respiratory specimens of infected patients. *N. Engl. J. Med.* **382(12)** (2020) 1177–1179.
[34] Y. Pan, D. Zhang, P. Yang, L.L.M. Poon and Q. Wang, Viral load of SARS-CoV-2 in samples. *Lancet* **20** (2020) 411–412.
[35] E.A. Meyerowitz, A. Richterman, R.T. Gandhi and P.E. Sax, Transmission of SARS-CoV-2: a review of viral, host, and environmental factors. *Ann. Intern. Med.* **174** (2020) 69–79.
[36] D. Kault, Superspreaders, asymptomatics and COVID-19 elimination. *Med. J. Aust.* **215** (2021) 140–140.e1.
[37] B. Ridenhour, J.M. Kowalik and D.K. Shay, Transmission of SARS-CoV-2: unraveling R_0: considerations for public health applications. *Am. J. Public Health* **104** (2014) e32–e41.